



Cross-kink unpinning controls the medium- to high-temperature strength of body-centered cubic NbTiZr medium-entropy alloy

Rajeshwar R. Eleti^{a,*}, Nikita Stepanov^a, Nikita Yurchenko^a, Sergey Zharebtsov^a, Francesco Maresca^b

^aLaboratory of Bulk Nanostructured Materials, Belgorod National Research University, Belgorod 308015, Russia

^bEngineering and Technology Institute Groningen, Faculty of Science and Engineering, University of Groningen, Groningen, the Netherlands

ARTICLE INFO

Article history:

Received 2 April 2021

Revised 19 October 2021

Accepted 20 October 2021

Available online 3 November 2021

Keywords:

High/medium-entropy alloys

Cross-kinks/jogs strengthening

Screw dislocations

Activation volume

ABSTRACT

The deformation mechanisms of a NbTiZr body-centered cubic (BCC) medium-entropy alloy (MEA) are investigated by tensile testing at various temperatures. The yield strength (YS) shows a strong temperature dependence from 77 K to 300 K, while being insensitive to temperatures between 300 K and 873 K, followed by a significant drop at 1073 K. TEM investigations show that the alloy deformation is controlled by screw-dislocation slip. Screw-dislocations with cross-kinks/jogs are frequently observed at all temperatures except at 1073 K. The deformed microstructure at 473 K reveals dislocations loops/debris indicating the dominance of cross-kink strengthening at moderate to high temperatures, leading to a temperature insensitive YS. The behavior of NbTiZr is consistent with the cross-kink strengthening mechanism, as also confirmed by the comparison between observed and predicted values of the activation volume. The TEM investigations at 1073 K are consistent with the annihilation of cross-kinks/edge dipoles, which can explain the observed strength drop above this temperature.

© 2021 Acta Materialia Inc. Published by Elsevier Ltd. All rights reserved.

In pure BCC metals, strength is controlled by the kink-pair nucleation and propagation mechanism, which is thermally activated. The kink nucleation barrier can be reduced by introducing solutes, as shown by atomistic analyses [1] and Monte Carlo simulation studies [2,3]. Maresca and Curtin [4] considered the interaction of screw dislocations with solutes in the context of concentrated alloys, like medium/high-entropy alloys (MEAs/HEAs) [5]. In [4], screw dislocations would spontaneously form kinked structures because of the exceptionally high solute-dislocation interaction fluctuations in the alloy. Because of this, instead of kink nucleation as in BCC metals or dilute alloys [1–3], kink migration or Peierls advancement would be the rate-controlling process in the complex concentrated BCC MEAs/HEAs at low to moderate temperatures.

The symmetry of the compact screw dislocation core structure in BCC metals induces spontaneous kinks on any of the three possible {110} slip planes containing the dislocation line [4], sometimes resulting in apparent {112}, {123} or pencil glide slip at the microscale [6]. Therefore, lateral kink migration on different slip systems leads to the collision of kinks travelling on different planes and the formation of cross-kinks, or jogs, that pin the dis-

location [4,7]. The break-away process of screw dislocations from cross-kinks requires the formation of vacancy and self-interstitial loops [4,8], hence the energy barriers controlling cross-kink unpinning depend on vacancy and self-interstitial formation energies [4,7,9]. Since these energies are large (several eV's), strength may become temperature-insensitive at moderate temperatures, where kink/Peierls strengthening becomes negligible, up to high temperatures.

Maresca and Curtin [4] showed that the theory of strengthening of screw dislocations could be used successfully for various BCC binary alloys, and for some concentrated alloys like MEAs/HEAs where edge dislocation strengthening is not significantly large [10]. In [4], the transition from low-T strengthening mechanisms (Peierls/kink migration) to the high-temperature cross-kink-dominated strengthening has been shown. However, a detailed comparison between the strengthening regimes predicted in [4] and experimental measurements of the activation volume and the dislocation structure as a function of temperature has not been performed yet. Here we perform this comparison for an equiatomic NbTiZr BCC-MEA, with focus on the cross-kink strengthening. In this alloy, yield strength predictions using the edge theory [11] show limited edge strengthening (refer supplementary file), hence strengthening is predicted to be controlled by screw dislocations as envisioned in [4].

* Corresponding author at: Laboratory of Bulk Nanostructured Materials, Belgorod National Research University, Pobeda 85, Belgorod, 308015, Russia.

E-mail address: rajeshwar.eleti@gmail.com (R.R. Eleti).

Table 1
Chemical composition of the as-cast equiatomic NbTiZr alloy.

	Nb	Ti	Zr	C	O	N
Composition	34.0 at.%	35.4 at.%	30.5 at.%	80 ppm	214 ppm	11 ppm

The constituent pure metals Nb, Ti, Zr (at least 99.95 wt.%) were used for vacuum arc-melting of the equiatomic NbTiZr MEA. The chemical composition of the as-cast ingot was analyzed using transmission electron microscopy (TEM, JEOL-JEM 2100) and interstitial impurities were quantified using the inert gas fusion method (Metec-300/600). Then, the as-cast alloy was cold-rolled until 80% height-reduction, annealed at 900 °C for 30 min, and water quenched. Tensile specimens having gage dimensions 6 (length) x 3 (width) x 1.5 (thickness) mm³ were cut from the annealed sheets. Tensile tests were performed in a temperature interval from 77 K to 1073 K in laboratory air for a constant 10⁻³ s⁻¹ strain-rate (Instron 5882). Each specimen was held for 15 min prior to the tensile test at the respective deformation temperature, to ensure homogeneous temperature throughout the specimen. Stress relaxation tests were performed during tensile deformation to investigate activation parameters that determine the rate-controlling mechanisms. The microstructural investigations were performed using electron back-scattering diffraction (EBSD) (FE-SEM, FEI-Nova NanoSEM 450) and TEM.

Table 1 shows the chemical composition of the as-cast NbTiZr alloy. The present as-cast alloy composition was close to the nominal composition of the equiatomic NbTiZr alloy. Further, the alloy consisted of a limited amount of interstitial impurities like C, O, and N.

Fig. 1(a) shows an EBSD-IPF map of a fully recrystallized microstructure of NbTiZr BCC-MEA with a grain size (d) ~ 50 μm. Engineering stress-strain curves at different temperatures and the effect of deformation temperature on the yield strength of NbTiZr BCC-MEA are shown in Figs. 1(b) and 1(c). The yield strength (YS, measured at $\sigma_{0.2\%}$) of the NbTiZr alloy decreases remarkably from 1410 MPa at 77 K to 630 MPa at 300 K. Then, an approximately plateau region is observed between 300 K and 873 K (Fig. 1(c)). Further temperature increase to 1073 K decreases the YS substantially. In Fig. 1(c) the compression data of NbTiZr reported by Senkov et al. [12] are also shown, together with the theory predictions of YS reported by Maresca and Curtin [4], that agree with the experiments. As apparent from Fig. 1(c), Senkov et al. [12] reports a significantly higher YS compared to our present tensile observations. The discrepancies might be attributed to a differences in response in compression with respect to tension, to the different specimen characteristics used by Senkov et al. [12] (rectangular compression specimen dimensions, 5 x 5 x 8 mm³) and by the rather coarse grains size, d ($d \geq 2$ mm), just resulting in 2 or 3 grains on the compression area of the specimens, thus yielding size effects and stronger orientation dependence. Finally, small compositional differences between the present alloy (34% Nb, 35.4% Ti, 30.5% Zr) and the one considered by Senkov et al. (35.6% Nb, 32.5% Ti, 31.9% Zr) may also contribute to yield strength differences. We have performed additional tests in compression at room temperature on the as-cast alloy to verify the discrepancies in the YS and found that the YS of NbTiZr was 695 MPa, which is still significantly lower than the value reported by Senkov et al. (ref. Supplementary materials). Maresca and Curtin [4] used Senkov et al. results to validate their proposed screw dislocation strengthening theory, by using two fitting parameters: the energy scale for solute-dislocation interaction fluctuations and the Peierls barrier for screw dislocation glide. We have verified that small adjustment in the fitted energy parameters can yield a very good match between Maresca and Curtin [4] theory and the present experiments.

Although it is now clear that there might be some differences between the Senkov et al. data and the ones measured in this work, the Maresca and Curtin theory predictions for this alloy are the ones reported in reference [4], which were fitted to Senkov et al. Thus, without adjusting/modifying the theory input parameters to match the present experiments, we have computed the contributions of the cross-kink and the Peierls-type mechanisms to the overall strength of the NbTiZr alloy, as shown in Fig. 1(c). First, the dominance of cross-kinks could be seen clearly above 400 K. Furthermore, the Peierls contribution to the overall strength is negligible above 400 K, but both the Peierls and cross-kink mechanisms contribute to the strength below 400 K. Adjustments of the input parameters of the screw dislocation theory to the current NbTiZr data would lower such transition temperature, consistent with the activation volume analysis (see discussion below).

Next, the NbTiZr alloy showed very good tensile ductility of at least 20% or higher, for any tested temperature. Furthermore, ductility increased with increasing temperature. However, the alloy showed limited strain-hardening, except at the 473 K and, yet slightly, at 673 K. Interestingly, in addition to notable strain-hardening, the stress-strain curve at 473 K showed serrations (see inset in Fig. 1(b)). To gain insight into the mechanical behavior of the alloy at 473 K, we performed an additional test at a lower strain-rate (10⁻⁴ s⁻¹). Fig. 2 shows the effect of the strain-rate on the tensile behavior of NbTiZr BCC-MEA at 473 K. The yield and flow stresses increase as the strain rate decreases, while the serrations become more frequent. As both the stress-strain curves appeared mostly parallel to each other, the strain-rate sensitivity was estimated for the YS as shown in the inset of Fig. 2. Here, a negative strain-rate sensitivity is found, $n_{SRS} = -0.051$. The occurrence of serrations and negative strain-rate sensitivity has been considered to be the classical signature of dynamic strain-aging (DSA), often referred to as Portevin-Lechatelier (PLC) effect [13–15]. It is noteworthy that the characteristics of the PLC effect in NbTiZr MEA were observed at temperature as low as 473 K (i.e., 0.17* T_m). Recently, Chen et al. [16] reported the above mentioned characteristics of the PLC effect in HfNbTaTiZr BCC-HEA at 673 K (i.e., 0.17* T_m). The possibility of long-range diffusion is highly unlikely in both the alloys to promote the PLC effect at such a low temperature. Serrations and nSRS or the PLC effect were also previously reported in dilute BCC alloys [17,18] and pure Fe consisting of interstitial solutes (including C) as low as 48 ppm [19–21], which is sufficient to induce the PLC effect below 473 K. Our present as-cast alloy consisted of C ~ 80 ppm, which was higher compared to the above noted studies. Therefore, the present experimental observations suggest that interstitial solutes like C and/or O strongly interact with dislocations and facilitate the occurrence of the PLC effect in NbTiZr BCC-MEA at 473 K.

The remarkable temperature-dependence of the YS indicated variations in the thermally-activated processes. We have estimated the activation volume (V^*) by performing stress relaxation tests during tensile deformation, to identify these processes. The details of evaluating V^* were described in our former article [22]. Fig. 1(d) shows the V^* values of NbTiZr as a function of YS at various deformation temperatures. In the same Figure, we have predicted the V^* values based on the screw dislocation strengthening theory [4] as follows. Above the transition temperature to fully cross-kink controlled strengthening (which theory predicts to be 420 K, see Fig. 1(c)), the activation volume of the full theory and cross-kink

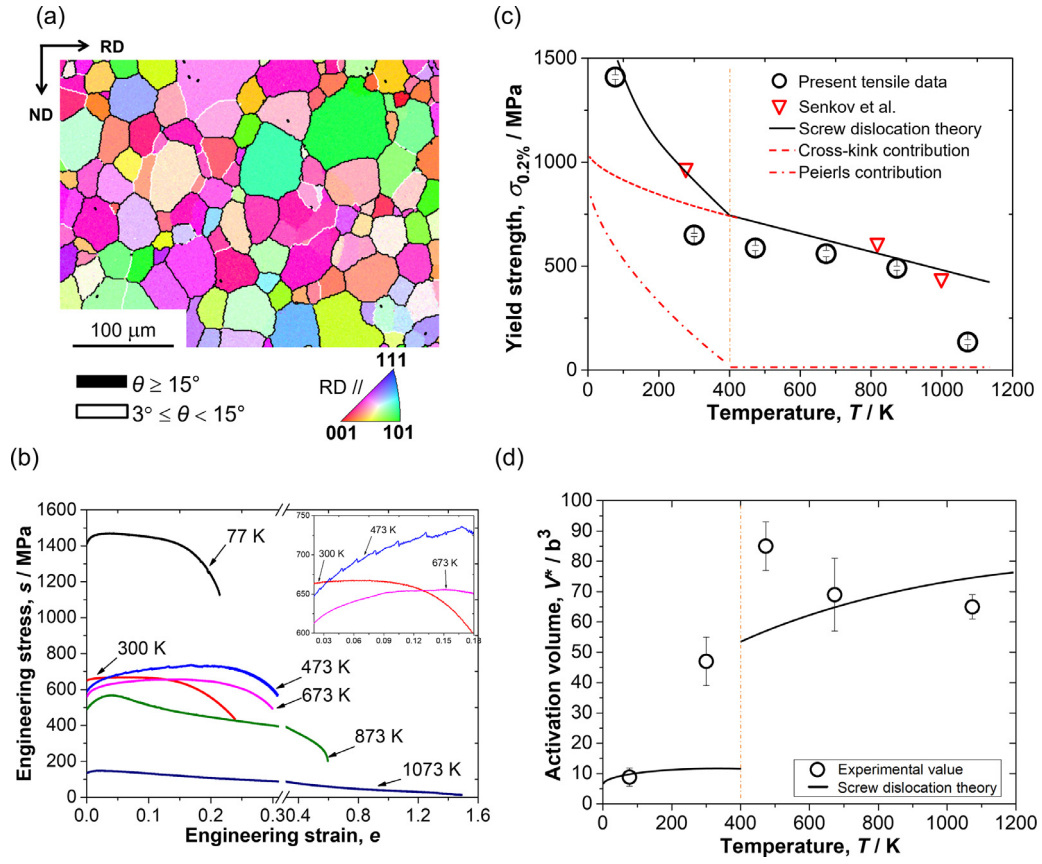


Fig. 1. Microstructure and stress-strain curves of NbTiZr during tensile deformation at different temperatures for the strain rate 10^{-3} s^{-1} . (a) EBSD-IPF map of fully recrystallized microstructure having grains size, $d \sim 50 \mu\text{m}$. (b) Tensile stress-strain curves of NbTiZr. Enlarged view of the stress-strain curves is shown in the inset of the figure. (c) Dependence of the yield strength (YS) as a function of deformation temperature. Strength contributions of cross-kink and Peierls mechanisms to the overall strength of NbTiZr was predicted with the screw strengthening theory by Maresca and Curtin [4]. (d) Dependence of the activation volume V^* on the temperature. V^* was measured at yielding ($\sigma_{0.2\%}$). The vertical dotted line in (c,d) represents a transition unto cross-kink mechanism.

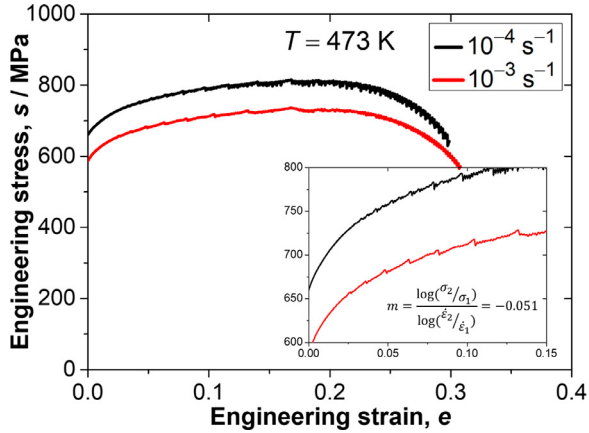


Fig. 2. Tensile stress-strain curves of NbTiZr deformed at 473 K for various strain rates. Enlarged view of the stress-strain curve and strain-rate sensitivity, m was evaluated using the formula shown in the inset.

contribution coincide and are computed as follows (by making use of Eq. 32 in [4]):

$$V^* = -\frac{\partial \Delta H}{\partial \tau} = \frac{3}{2} \frac{E_i}{\tau_{xk,0}} \left[\frac{k_B T}{E_i} \ln \left(\frac{\dot{\epsilon}_0}{\dot{\epsilon}} \right) \right]^{1/3} \quad (1)$$

where E_i is the self-interstitial formation energy, which is the relevant energy controlling cross-kink strengthening in this alloy, $\tau_{xk,0}$ is the $T = 0 \text{ K}$ stress for breaking the cross-kinks, k_B is the Boltz-

mann constant, T is the absolute temperature, $\dot{\epsilon}_0$ is a reference strain rate and $\dot{\epsilon}$ is the experimental strain rate. All the values of the input quantities in (1) are those specified in [4], hence they are not repeated here. Below this transition temperature, the Peierls mechanism (see [4]) is also operating. Since the strengthening contributions of cross-kink and Peierls mechanisms sum up, we can compute the activation volume as follows [23],

$$V^* = \left(\frac{1}{V_{xk}^*} + \frac{1}{V_p^*} \right)^{-1} \quad (2)$$

where V_{xk}^* is calculated according to (1) and V_p^* is the Peierls contribution calculated by making use of Eq. 32 in [4]

$$V_p^* = \frac{3}{2} \frac{\Delta E_{b,p}}{\tau_{p,0}} \left[\frac{k_B T}{\Delta E_{b,p}} \ln \left(\frac{\dot{\epsilon}_0}{\dot{\epsilon}} \right) \right]^{1/3} \quad (3)$$

where $\Delta E_{b,p}$ is the energy barrier for the Peierls mechanism and $\tau_{p,0}$ the associated $T = 0 \text{ K}$ Peierls stress (accounting for solute fluctuations), both defined in [4], and the rest of the input has the same meaning as specified next to Eq. (3). All the necessary theory input is reported in Table 2 of Ref. [4] for the equiatomic NbTiZr alloy. As discussed in [8], the required energy for the creation of self-interstitials is much greater than vacancies. As estimated in [4] by using Zhou et al. [24] interatomic potentials, the self-interstitial formation energy $E_{si}=3.535 \text{ eV}$ is almost twice the vacancy formation energy $E_v=1.868 \text{ eV}$.

The predicted V^* values (Fig. 1(d)) are overall consistent with the experiments, showing that the cross-kink strengthening mechanism can indeed be the controlling strengthening parameter at

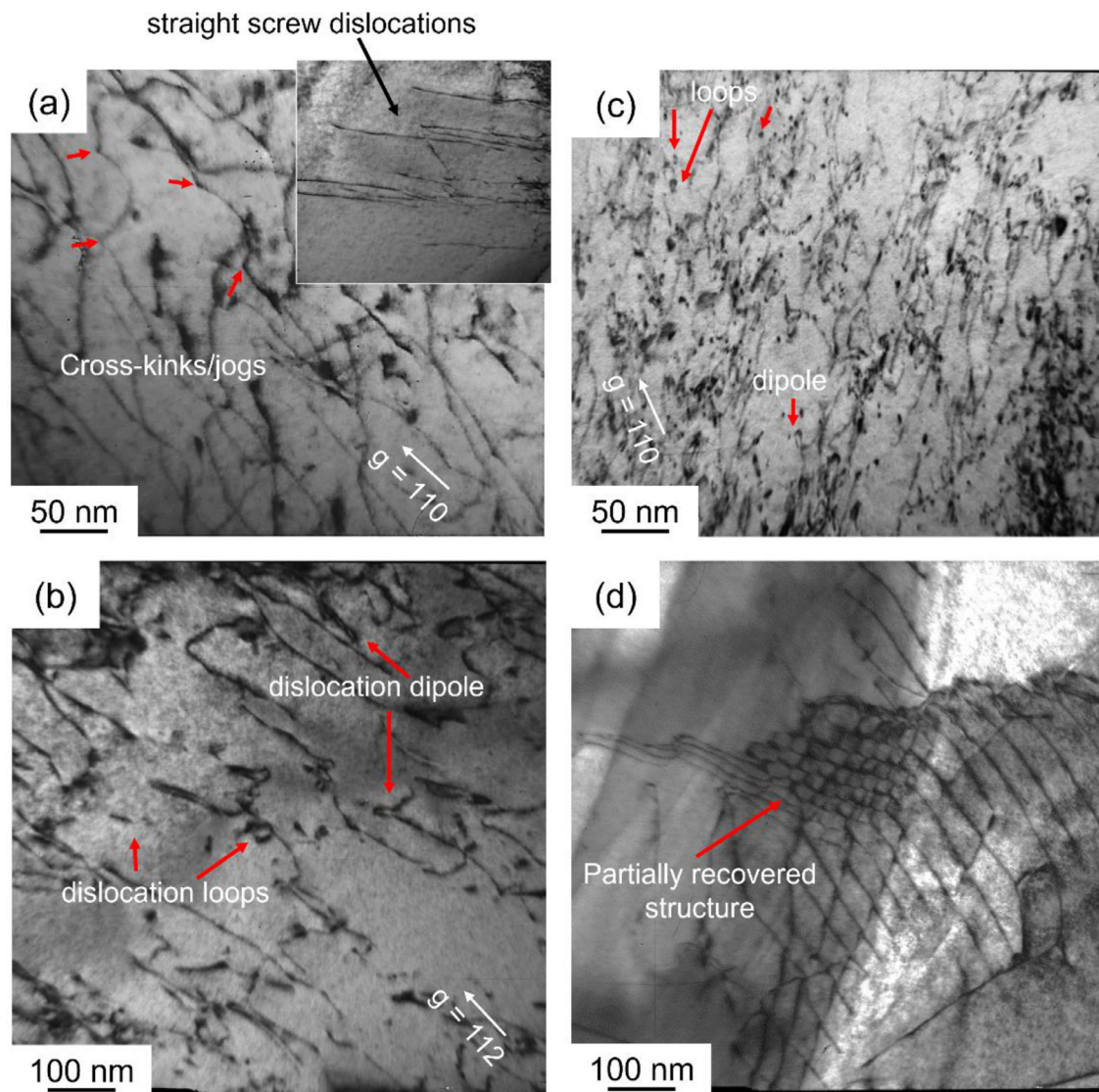


Fig. 3. (a-d) Microstructural investigation of NbTiZr deformed at different temperatures. (a) 77 K, (b) 300 K, (c) 473 K, (d) 1073 K.

elevated temperatures. The experimentally measured $V^* \sim 8 b^3$ at 77 K is consistent with the Peierls mechanisms controlling the low temperature strength. $V^* \sim 47 b^3$ at 300 K indicates that dislocation glide might be fully controlled by the cross-kink strengthening mechanism already at this temperature, which can be predicted by minute adjustment of the theory input. At any rate, the screw theory does predict correctly a transition from Peierls to cross-kink controlled activation volume at increasing temperature. The overall trend of activation volume V^* is also captured by the theory and thus can be explained as cross-kink strengthening. The sharp increment of V^* at 473 K is not explained by the current theory, and we argue that this might be connected to PLC (see previous discussion). This aspect requires a separate, detailed analysis that is left to future study. At high temperature (1073 K) the activation volume is overestimated and the cross-kink strengthening mechanism also overestimates the experimental yield strength. Maresca and Curtin consider that cross-kink strengthening is not operating above $0.5 \cdot T_m \sim 1140$ K because of enhanced vacancy diffusion. Rao et al. [9] estimate an annihilation of the edge dipoles originating from the cross-kink unpinning at a temperature between 1015 K and 1130 K for the equiatomic NbTiZr alloy, therefore encompassing the 1073 K temperature at which the strength drop is observed.

Next, in order to verify the predicted deformation mechanisms, microstructural investigation using TEM was performed on specimens of NbTiZr BCC-MEA undergoing tensile deformation at various temperatures up to small global uniaxial strains, $\varepsilon = 2 \sim 3\%$ (Fig. 3). At 77 K and 300 K, the dislocation morphology revealed cross-kinks/jogs (edge-dipoles) on screw-dislocations (Fig. 3(a,b)). At 77 K, very straight and long screw dislocations could be observed. Also, TEM investigation revealed that deformation occurred only by dislocation slip, since no traces of deformation twinning was observed. At 473 K, TEM images revealed a significant fraction of dislocation debris and loops. At yet higher temperatures (1073 K), the microstructure showed dislocations arranged into a honeycomb-like structure, presumably formed due to the activation of recovery processes like dislocation climb. Furthermore, dislocations in the unrecovered regions were predominantly straight, and lacked cross-kinks, unlike the dislocation morphology at lower deformation temperatures. Moreover, no dislocation debris or loops were found after deformation at 1073 K. These high-temperature observations confirm our previous analysis and the mechanisms predicted by Maresca and Curtin [4].

The observed straight dislocations and debris at low temperatures (77 K) are consistent with the screw dislocation theory pre-

diction of cross-kink and Peierls strengthening as the controlling mechanisms of screw dislocation strength at low temperatures. At moderate temperatures (300 K, 473 K), the presence of less straight segments and the dominance of debris and dislocation loops behind the dislocations confirm that cross-kink strengthening is the controlling strengthening mechanism as temperature increases. Rao et al. [25] referred to a transition to a similar mechanism (edge-dipole strengthening) with increasing temperature. Screw dislocations must break-away or disentangle from the cross-kinks to move forward. According to MD simulation studies on pure Fe (α -Fe) reported by Marian et al. [7], as well as by the MD simulations on a model NbTaV BCC-MEA shown in Maresca and Curtin [4], the combination of kink pairs on two adjacent planes allows the dislocation to reconnect on a single plane. In the wake of reconnection, the cross-kinks transform into dislocation loops around vacancies or interstitials, resulting into debris that is left behind the screw dislocation after it has disentangled. Although atomistic-scale observations of the deformation mechanism of NbTiZr could not be performed here, the above considerations from Marian et al. [7] and Maresca and Curtin [4] agree with the microstructural evidence shown in Fig. 3(b,c). Above 300 K, since the strength of NbTiZr is controlled by cross-kinks, the break-away energy barrier of screw dislocations off the cross-kinks can be very large. Due to this, the strength of the alloy becomes almost insensitive to the deformation temperature leading to a plateau region, as observed in Fig. 1(c). Furthermore, Rao et al. [25] and Maresca and Curtin [4] argued that the NbTiZr may have a critical temperature close to $0.5 \cdot T_m$, where diffusion related processes become important. According to Maresca and Curtin, at high temperatures, the vacancy cross-kinks can be mobile enough to glide along the screw dislocation, eventually leading to annihilation (vacancy cross-kinks annihilating with self-interstitial cross-kinks) and the loss of strength. Rao et al. argued that, at high temperatures, edge dipoles dragging from cross-kinks would annihilate due to climb, and their estimated annihilation temperature range for the equiatomic NbTiZr alloy (1015 K and 1130 K) is consistent with the straight, smooth, and long screw dislocations observed at 1073 K in this study. Also, the microstructure at 1073 K revealed the possibility of diffusional processes like dynamic recovery. The transition from cross-kink strengthening mechanism to high temperature glide is smooth and not affecting the dislocation velocities significantly, within the temperature range explored here.

To summarize, the mechanical behavior of an equiatomic NbTiZr BCC-MEA was systematically investigated in a temperature interval from 77 K to 1073 K. The YS of NbTiZr alloy showed strong temperature dependence from 1410 MPa at 77 K to 630 MPa at 300 K. The YS was almost independent of the deformation temperature between 300 K and 873 K, but was followed by a significant drop at 1073 K. Results at 473 K also show the occurrence of serrations and negative strain-rate sensitivity, presumably due to the presence of interstitial impurities like C or O. Microstructural investigations revealed that plastic deformation occurred only by dislocation glide with no twinning involved, and was controlled by screw dislocations. Most notably, the present experimental observations suggest that cross-kink unpinning is the controlling strengthening mechanism at intermediate to high temperatures, thus validating the theoretical results of Maresca and Curtin [4]. At low temperatures (77 K), the screw-dislocation motion is controlled by different mechanisms: the measured activation volume is consistent with a combination of Peierls advancement and cross-kink strengthening. At moderate temperatures (300–873 K), the disentanglement of cross-kinks controls the screw-dislocations

glide, as confirmed by the comparison between the theoretical predictions of the activation volume and the experimental measurements, including extensive observation of debris behind the dislocations. Straight dislocations glide as straight segments at temperatures above 1073 K. The present experiments show evidence of cross-kink annihilation, that leads to an abrupt loss of YS, thus confirming the analysis of Maresca and Curtin [4] and the predictions of Rao et al. [25].

Declaration of Competing Interest

The authors declare that they have no known competing financial interests or personal relationships that could have appeared to influence the work reported in this paper.

Acknowledgements

The authors gratefully acknowledge the financial support from the Russian Science Foundation Grant no. 19-79-30066. The authors are grateful to the personnel of the Joint Research Center, "Technology and Materials", Belgorod National Research University, for their assistance. The authors would like to extend acknowledgements to Dr. D. Shaysultanov of Laboratory of Bulk Nanostructured Materials, Belgorod National Research University for his assistance during the experiments. The authors would like to acknowledge the fruitful comments of the anonymous reviewers that greatly contributed to the improvement of this work.

Supplementary materials

Supplementary material associated with this article can be found, in the online version, at doi:[10.1016/j.scriptamat.2021.114367](https://doi.org/10.1016/j.scriptamat.2021.114367).

References

- [1] D.R. Trinkle, C. Woodward, *Science* 310 (80) (2005) 1665–1667.
- [2] Y. Zhao, J. Marian, *Model. Simul. Mater. Sci. Eng.* 26 (2018) 45002.
- [3] S. Shinzato, M. Wakeda, S. Ogata, *Int. J. Plast.* 122 (2019) 319–337.
- [4] F. Maresca, W.A. Curtin, *Acta Mater* 182 (2020) 144–162.
- [5] J.-W. Yeh, S.-K. Chen, S.-J. Lin, J.-Y. Gan, T.-S. Chin, T.-T. Shun, C.-H. Tsau, S.-Y. Chang, *Adv. Eng. Mater.* 6 (2004) 299–303.
- [6] C. Du, F. Maresca, M.G.D. Geers, J.P.M. Hoefnagels, *Acta Mater* 146 (2018) 314–327.
- [7] J. Marian, W. Cai, V.V. Bulatov, *Nat. Mater.* 3 (2004) 158–163.
- [8] G.J. Ackland, D.J. Bacon, A.F. Calder, T. Harry, *Philos. Mag. A* 75 (1997) 713–732.
- [9] J. Chaussidon, M. Fivel, D. Rodney, *Acta Mater* 54 (2006) 3407–3416.
- [10] C. Lee, F. Maresca, R. Feng, Y. Chou, T. Ungar, M. Widom, K. An, J.D. Poplawsky, Y.-C. Chou, P.K. Liaw, W.A. Curtin, *Nat. Commun.* 12 (2021) 5474.
- [11] F. Maresca, W.A. Curtin, *Acta Mater* 182 (2020) 235–249.
- [12] O.N. Senkov, S. Rao, K.J. Chaput, C. Woodward, *Acta Mater* 151 (2018) 201–215.
- [13] L.P. Kubin, Y. Estrin, *Acta Metall.* 33 (1985) 397–407.
- [14] J.M. Robinson, M.P. Shaw, *Int. Mater. Rev.* 39 (1994) 113–122.
- [15] J.M. Robinson, *Int. Mater. Rev.* 39 (1994) 217–227.
- [16] S. Chen, W. Li, F. Meng, Y. Tong, H. Zhang, K.-K. Tseng, J.-W. Yeh, Y. Ren, F. Xu, Z. Wu, P.K. Liaw, *Scr. Mater.* 200 (2021) 113919.
- [17] Y. Zhao, L. Dezerald, M. Pozuelo, X. Zhou, J. Marian, *Nat. Commun.* 11 (2020) 1227.
- [18] L.A. Gypen, A. Deruyttere, *J. Less Common Met.* 86 (1982) 219–240.
- [19] E. Pink, S. Kumar, *Mater. Sci. Eng. A* 201 (1995) 58–64.
- [20] D. Caillard, J. Bonneville, *Scr. Mater.* 95 (2015) 15–18.
- [21] J.D. Baird, *Metall. Rev.* 16 (1971) 1–18.
- [22] R.R. Eleti, N. Stepanov, N. Yurchenko, D. Klimenko, S. Zhrebtsov, *Scr. Mater.* 200 (2021) 113927.
- [23] G. Laplanche, J. Bonneville, C. Varvenne, W.A. Curtin, E.P. George, *Acta Mater* 143 (2018) 257–264.
- [24] X.W. Zhou, R.A. Johnson, H.N.G. Wadley, *Phys. Rev. B* 69 (2004) 144113.
- [25] S.I. Rao, C. Woodward, B. Akdim, E. Antillon, T.A. Parthasarathy, O.N. Senkov, *Scr. Mater.* 172 (2019) 135–137.